A STUDY OF THE EFFECTS OF GEOMETRIC IMPERFECTION UPON THE STABILITY BEHAVIOR OF CYLINDRICAL SHELLS UNDER AXIAL COMPRESSION

A THESIS

Presented to

The Faculty of the Division of Graduate

Studies and Research

by

Michael Fee Duggan

In Partial Fulfillment

of the Requirements for the Degree

Master of Science

in the School of Aerospace Engineering

Georgia Institute of Technology

December 1971

A STUDY OF THE EFFECTS OF GEOMETRIC IMPERFECTION UPON THE STABILITY BEHAVIOR OF CYLINDRICAL SHELLS UNDER AXIAL COMPRESSION

Approved: [signature]

Chai[illegible]

Date approved by Chairman: 11/22/71

ACKNOWLEDGMENTS

I wish to express my deapest appreciation to my advisor, Dr. James I. Craig, for his many hours of advice and assistance without which this thesis would never have been completed. Also appreciated is the encouragment he has given in other areas of my work and interest.

I am also greatful to Professor W. H. Horton and R. L. Carlson for their gracious consent to read and edit this thesis and for their helpful suggestions in making this work complete.

This work was sponsored in part by NASA Grant No. NGR 11-002-096 and Grant AFOSR 68-1476, and I am again indebted to Professor W. H. Horton for the opportunity to conduct this research.

TABLE OF CONTENTS

LIST OF TABLES

LIST OF ILLUSTRATIONS

LIST OF SYMBOLS

e	the eccentricity introduced into the circularity data due to specimen positioning error
LVDT	linear variable differential transformer
R_θ	the measured radius from the mounting axis to the shell skin
R	the radius from the true center to the skin
θ	the angular position of the circularity scanning transducer from an established zero reference on the specimen
A_0, A_1, B_1	fourier coefficients
φ	phase angle
$F(e_n)$	the component of mounting eccentricity present in the data at a particular angular position
w	lateral displacement
Q	concentrated lateral load
L	column length
E	Young's Modulus
P	compressive load on a column
K_1	lateral stiffness as determined analytically
a, b	length of sides of a rectangular plate
N_x	inplane compressive loading acting upon a rectangular plate
d_1	the deflection across the load transducer
d_2	traverse table motion
δ	shell wall deflection

DEFINITIONS

Geometric Imperfections	- geometric deviation from an ideal shape
Mounting Axis	- the real axis about which the specimen revolves during circularity measurement
True Center	- the geometric center of the specimen at an axial station
Perfect Shell Axis	- the axis of that perfect circular cylinder which best approximates the geometry of the real specimen
True Eccentricity	- the variation of the true center from the perfect shell axis at an axial station

SUMMARY

This thesis is a study of the initial geometry and lateral stiffness of circular cylindrical shells. A nondestructive test program for the determination of stability loads of cylindrical shells is pursued through two approaches.

A detailed study of the initial geometries of large and small scale specimens is presented. The initial stiffness configuration of the small shell is investigated, this specimen having been selected for detailed study. An evaluation is made of the effect of geometric irregularity upon the initial stiffness.

The behavior of the specimen lateral stiffness under compressive loading is investigated, and it is demonstrated that buckling loads can be predicted for monocoque shells by this method. A new technique is introduced, employing a Southwell analysis of the lateral load - deflection data, which concurs with the previous method. This new approach greatly reduces the compressive load necessary for accurate prediction.

CHAPTER I

INTRODUCTION

The cylindrical shell under axial compression, more than any other structure, has shown large discrepancy from theoretical prediction. Nondestructive skin wrinkling was tolerable in the early years of slow speed flight but with the advent of vehicle velocities substantially exceeding sonic speeds, this behavior could no longer be tolerated. Increased wall thickness was, of course, one solution but increased weight is the penality. The elusive goal, which has been sought since those early days, is an efficient combination of high strength, minimum weight, and accurately predictable stability limits.

The classical formulas for the stress distribution in a uniformly compressed circular cylinder were calculated as early as 1908 by Rudolf Lorenz and in 1910 by S. Timoshenko (1). Serious doubts arose as to the validity of the theory when later experimental results revealed buckling loads which were consistently a fraction of the predicted values. Slight discrepancies in construction of seemingly identical specimens were apparently capable of producing large variations in their buckling loads.

R. V. Southwell (2) is generally credited with producing the first experimental technique capable of accurately and nondestructively predicting the critical load of a column. Later work has shown the "Southwell plot" method applicable to the flat plate, the cylindrical

shell, and other stability problems (3). In practice, the method yields accurate critical load predictions for many stability problems. The procedure has not, however, been satisfactorily applied in a direct manner to the stability problem of an unstiffened, isotropic cylindrical shell under axial compressive load. Several investigators have used elaborate harmonic analysis schemes to "filter" data from large portions of the shell and have interpreted the results by the Southwell plot procedure (4,5,6). It has not, however, been possible to apply the procedure directly on a pointwise basis to the shell problem.

Structural stiffness has long been recognized as a possible criterion for stability prediction (7,8). Most investigations have, however, ignored the potential of this approach and have been concerned instead with a direct correlation of collapse load with prediction or more recently with the aforementioned Southwell plot procedure, leaving the stiffness behavior largely unexplored.

This thesis is an effort to study in an experimental manner the variation in lateral stiffness of the wall of circular cylindrical shells, and the behavior of this stiffness with increasing levels of axial compression. The initial lateral stiffness of the wall of a virgin monocoque cylindrical shell has been mapped and correlation with the initial geometry attempted. A technique outlined by Bank (9) is applied to extrapolate critical axial load from the behavior of lateral stiffness under less than critical compressive loads. This method is extended and a potentially powerful new procedure to estimate critical loads is presented.

The stiffness determinations used in this work are static in nature, employing load-deflection data due to small test forces applied normal to the shell wall at the point of interest. It is acknowledged that a dynamic approach should yield similar results, but it must also be recognized that application of dynamic tests can involve substantial increases in complexity over the static test. No attempt to use dynamic procedures has been made in this work.

CHAPTER II

INITIAL SPECIMEN GEOMETRY ANALYSIS

The results of early stability tests upon circular cylindrical shells raised questions as to the validity of the theory which was generally accepted. It was realized that other factors, too detailed in nature to be easily treated in theory, must then influence the behavior of the shell. These factors, usually termed imperfections, were thrown to the experimentalist to identify. The conclusion of many investigators is that geometric imperfections - deviations from an ideal shape - are a prime factor contributing to the discrepancy between experimental and theoretical results. It is this aspect which is now to be investigated.

In order to determine the undeformed shape of large and small scale thin walled circular cylindrical shells, a technique was devised to measure the specimen circularity at various positions along the shell axis. However, the initial inability to position the mounting (rotation) axis coaxially with the specimen axis unavoidably introduced an artificial eccentricity error into the data. To determine the true shape of the specimen it was necessary to identify - and remove - this undesired component of the data.

The initial geometry of two distinct shell size classes was studied, and a comparison of the results was later made to decide the course of the experimental program. The large specimen was the

first to be studied.

Large Scale Specimens

It was decided to investigate the initial geometry of a class of large (nine foot length, six foot diameter) circular cylinders manufactured for axial compressive stability studies to be performed at the Georgia Institute of Technology Aerospace Department. With this information, correlation of data from numerous smaller specimen tests could be attempted with initial geometry as a common criterion.

Data Recording

The specimen was mounted in a configuration which allowed axial rotation only, so that radial displacements might be measured. Since the true center of the shell was unknown at the ends, the mounting points of the rotation frame did not coincide exactly with the axis of the specimen. This resulted in an unknown mounting eccentricity, e, being added vectorially to all measurements.

A single linear variable differential transformer (LVDT) was used as the transducer for all displacement measurements in the test. To establish a known measurement reference, a ten foot precision straight edge was positioned outside the shell and parallel to the mounting axis. The LVDT was then attached to the straight edge in such a manner that it could be positioned along the specimen axis as desired.

Angular Position Measurements. The schematic diagram, Figure 1, depicts the shell scan and data recording arrangement. The Hewlett-Packard 2115A digital computer was the principle coordinating device

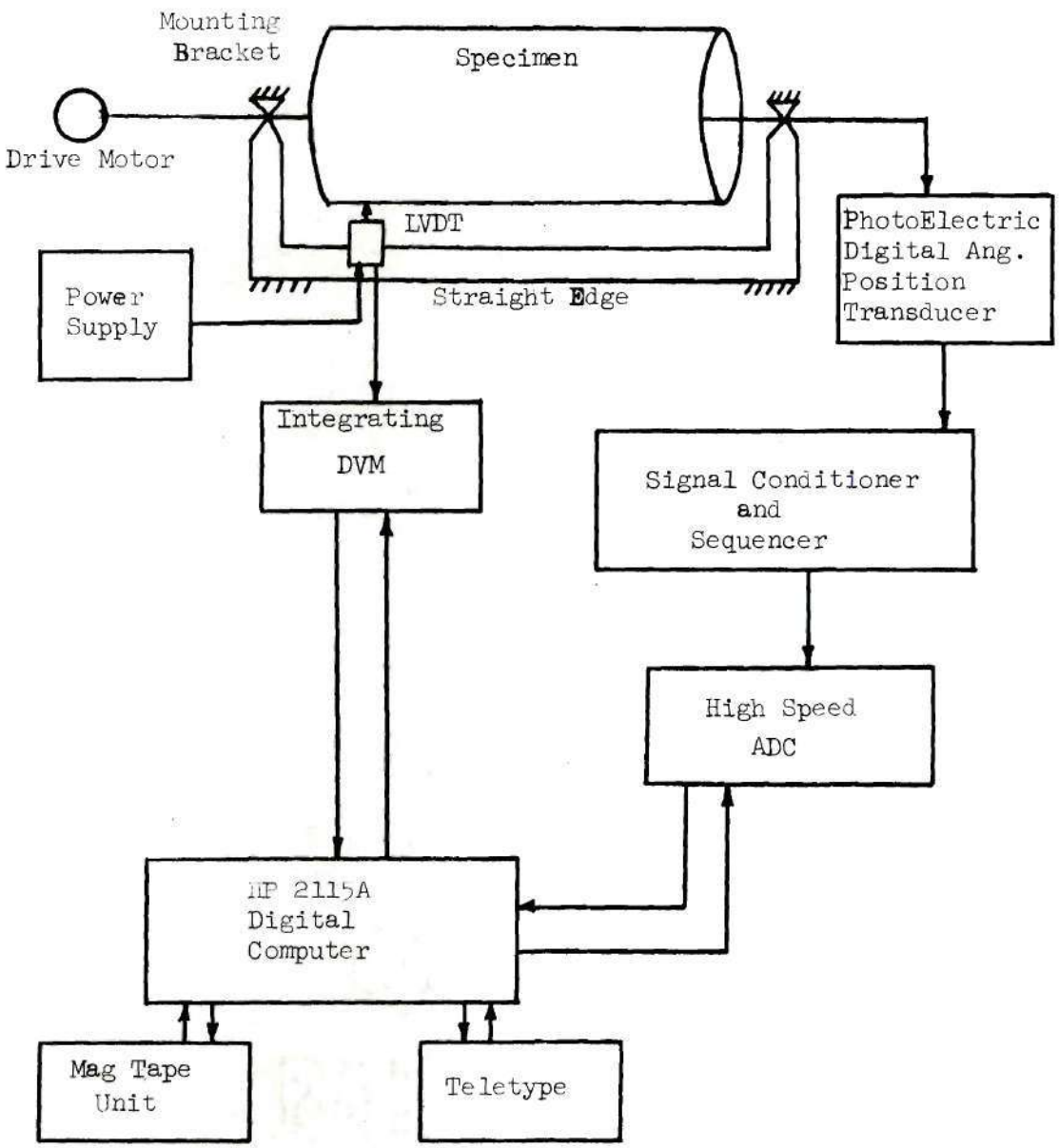

Figure 1. Data Recording System Schematic Diagram

of the data scan operation. As the specimen was rotated, the angular position transducer supplied pulses every one degree starting at an established zero degree reference position. These pulses were transformed to a digital equivalent by the analog-to-digiral converter (ADC). The computer interrogated the ADC and encoded the digital voltmeter (DVM) on ever second ADC pulse (two degree intervals). The DVM output representing displacement transducer readings was processed in the computer and stored in memory. At the completion of a 360 degree scan the data could be written as a record on digital magnetic tape if all systems performed properly or disregarded and a new scan initiated. Circularity measurements of the specimen at as many axial stations as desired could be performed on the shell to generate the necessary data.

Data Reduction

The desired result of the measurement program is the deviation of the real shell from a perfect cylinder of the same average radius. The process of describing the real shell and determining this deviation, or imperfection, can be classified into three main groups:

1. Mounting eccentricity identification.
2. Identification of the true center location at each axial station.
3. Location of the perfect shell axis.

Mounting Eccentricity (1). The radial measurement data for each axial station was represented by a Fourier series over an interval equal to the circumference. There are several justifications for describing the data in this manner. If the measurements of a 360

degree scan are plotted in cartesian coordinates, the radial values vary sinusoidally about a mean value. A mounting induced eccentricity can be shown to alter the data only in the first harmonic sine and cosine terms. Figure 2 shows the geometry associated with the shell measuring system where R_θ is the measured radius from the mounting axis to the shell skin, R is the radius to the true center of the shell at the particular axial station, and e the added mounting eccentricity.

The law of cosines is applied to solve for R_θ in terms of R, e and θ .

$$R^2 = R_\theta^2 + e^2 - 2R_\theta e \cos(\pi-\theta)$$

solving for R_θ

$$R_\theta = e \cos(\pi-\theta) \pm \sqrt{R^2-e^2 \sin^2(\pi-\theta)}$$

and for $R^2 >> e^2$

$$R_\theta \cong R - e \cos(\pi-\theta)$$

As θ varies from zero to 2π, the average value of the term

$$e \cos(\pi-\theta)$$

is zero. Thus

$$[R_\theta]_{avg} = [R-e \cos(\pi-\theta)]_{avg} = [R]_{avg} - [e \cos(\pi-\theta)]_{avg} = R_{avg}$$

for the shell.

The significance of this relationship is realized if a perfectly circular cylindrical shell were eccentrically mounted and scanned in the manner previously described. The data values would obviously vary sinusoidally about a mean value with a single maximum and minimum point on the interval defined by the circumference. The Fourier representation of this data would appear as follows:

$$R_\theta = \frac{A_o}{2} + A_1 \cos \frac{2\pi i}{180} + B_1 \sin \frac{2\pi i}{180}$$

$$i = 1 \text{ to } 180$$

This expression could be written as

$$R_\theta = \frac{A_o}{2} + e \cos(\pi-\theta+\varphi)$$

where

$$e^2 = A_1^2 + B_1^2$$

and

$$\varphi = \text{Arctan} \frac{A_1}{B_1}$$

The result shows that the mounting eccentricity affects the measurements with the addition of first harmonic trigonometric terms. Since all irregularities inherent to the specimen must influence the higher harmonic terms of the infinite series (a real shell would require an infinite series representation), the mounting eccentricity is immediately identified.

Included with the coefficients of a function represented by a Fourier series is a zero frequency term representing the average value of that function over the interval. For the shell this term is the mean radius at that station and is independent of mounting eccentricity.

True Centers (2). The eccentricity has been identified as the sum of the first sine and cosine terms of the series representation. If i denotes angular position of a transducer reading and n the axial station of the complete scan containing the i^{th} reading, then $F(e_n)$ - the component of the mounting eccentricity present in the data - can be written in the following form.

$$F(e_n) = A_{1_n} \cos \frac{2\pi i}{180} + B_{1_n} \sin \frac{2\pi i}{180}$$

for i = 1 to 180

Since the maximum value of $F(e_n)$ occurs at $\pi/2 - \varphi$ radians, then this angle is the direction of the eccentricity from the n^{th} mounting axis center. At this angular position the true center is on a radial line, and a distance e_n, from the rotation (mounting axis) center. For the present problem a cartesian representation of the coordinates of the true center is best suited for later analysis. Thus, the true center for the n^{th} axial station can be represented in carestian form as follows.

$$X_n = e_n \cos \left(\frac{\pi}{2} - \varphi_n\right)$$

$$Y_n = e_n \sin \left(\frac{\pi}{2} - \varphi_n\right)$$

The coordinate system is shown in Figure 3.

Perfect Shell Axis (3). The true centers calculated for each axial station need not be coincident. This is obviously the case if the shell were slightly bowed or corkscrewed along its axis. The requirement now is to determine the ideal circular cylinder which best

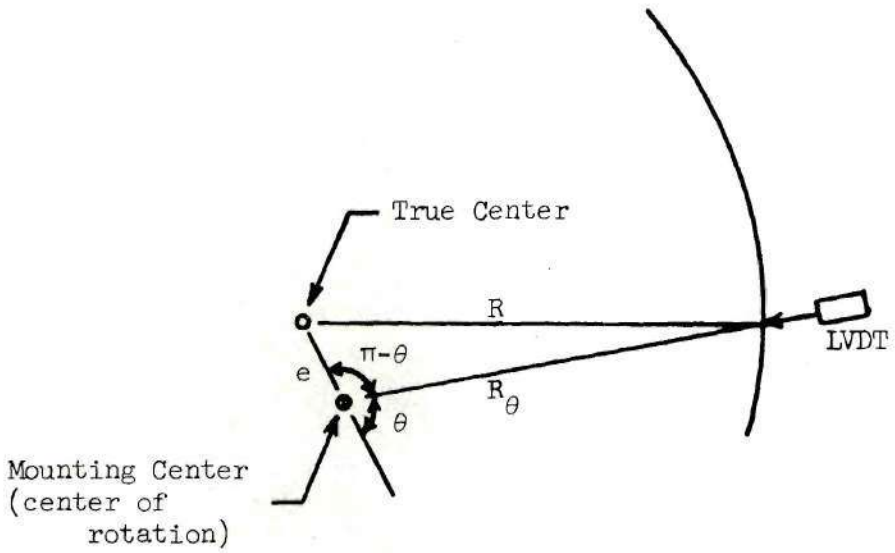

Figure 2. Specimen Measurement System Geometry

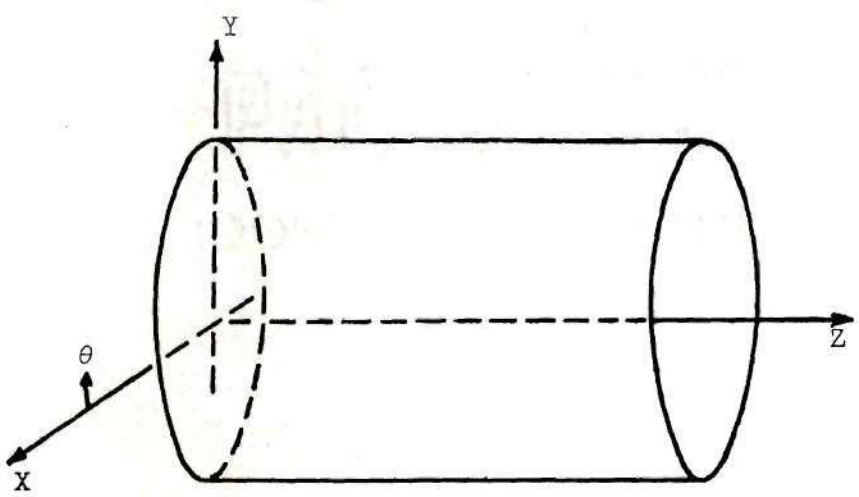

Figure 3. Eccentricity Analysis Coordinate System

approximates the data. The radius of this imaginary shell would be the average radius of the real specimen, but the location of its axis must be determined. If a linear least squares fit is performed upon the previously calculated true centers, then a shell with this line as its axis and the average radius previously calculated is, by definition, that perfect cylinder which best approximates the real shell. The calculation process is as follows.

Each station true center can be projected into the orthogonal coordinate planes. A first order least square fit is then performed separately on the points in these two planes. This results in two linear equations, each functions of axial position. Thus the position of the perfect shell center - for any axial station - is the square root of the sum of the squares of the functional values for the two equations in the orthogonal planes.

The deviation of the true centers from the perfect shell axis gives rise to what might best be described as the true or inherent eccentricity - the variation of the true center from the perfect shell axis at an axial station. This eccentricity is the result of geometric irregularity of the specimen and is characteristic of the amount of imperfection inherent in the real shell.

Computer programs to perform the processes discussed are located in the appendix.

Analysis of Results

The results of the data scan and reduction processes can best be represented in graphical form, as depicted in Figure 4. This figure is a partial representation of the shell, each trace representing a 360

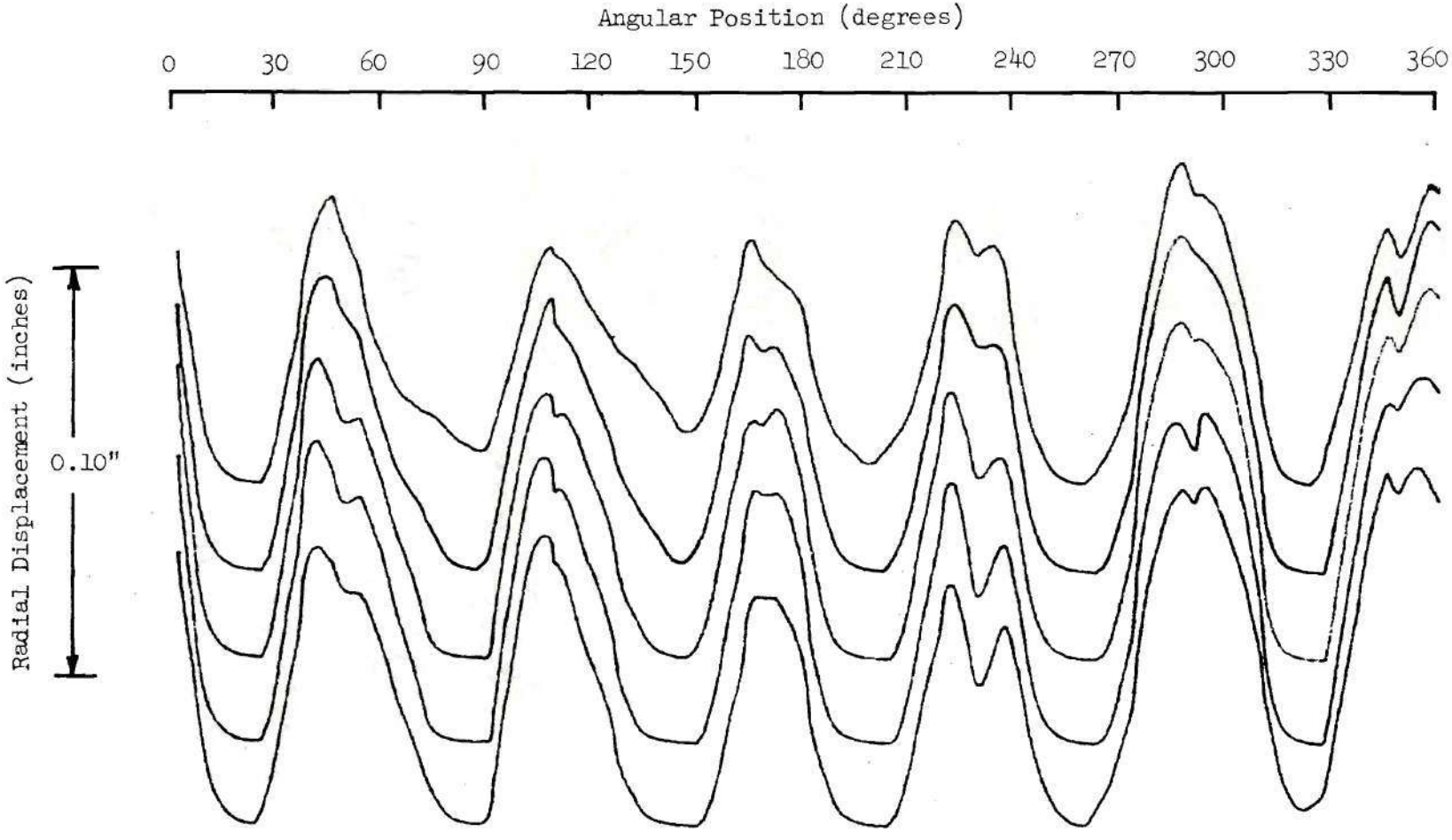

Figure 4. Large Shell Initial Geometry

degree scan at equally spaced intervals along the axis. Successive traces are shifted vertically in direct proportion to their axial position in an attempt to add some "perspective" to the representation. A measure of radial deviation is indicated by the 0.10 inch var. These plots were generated from the shell geometry data previously stored on magnetic tape. Data was processed by the 2115A computer and subsequently plotted under direct computer control on a Hewlett-Packard 7004A X-Y recorder.

The specimen was constructed of six curved panels joined lengthwise by lap seams and held circular by rigid end-rings. This construction is evident on the plots, with six peaks indicating the seam locations and the panel interiors as apparent valleys. These regions of apparent negative curvature are actually areas of relative flattness with respect to the average radius and may represent significant geometric imperfection. The lap type seam is very effective in maintaining a straight generator in that vicinity of the shell. The interior panel regions, especially near the shell mid-axis region, tend to have shorter radii and give rise to a "reverse barrel" shape. This is the anticlastic curvature found in many curved structures formed from originally flat materials.

Small Scale Specimens

The unique advantages of scale model test programs have long been recognized by engineers as a desirable alternate for often difficult, complex and expensive full scale testing. The wind tunnel aerodynamic test model and the photoelastic structural test model are perhaps the

best examples of this technique. The efficiency of this approach has not been lost in shell stability tests. Moderate sized acrylic plastic stiffened shells have recently been studied with notable success at Georgia Tech (6).

The most troublesome feature of small scale shell stability testing is, however, the generally unresolved question as to how well the model represents the full scale vehicle from the point of view of initial imperfections - both geometric and material. The present work is directly concerned with assessing the degree of imperfection present and its effect on the stability limit. To develop a basis for comparison with the full scale vehicle a small plexiglass monocoque cylinder was fabricated (Figure 5). This specimen was subjected to a scanning procedure similar to that outlined for the large shell and a quantitative measure of the initial geometry determined.

Scanning Procedure

The displacement scanning technique outlined previously for the full scale vehicle can be directly applied to the small scale study. The appreciable reduction in specimen size simplified the mechanics and permitted the cylinder to be mounted in a more convenient vertical configuration. The specimen was mounted coaxially on a rotating table as shown in Figure 5 and supported by a precision bearing. A mounting rail fixed vertical and parallel to the table axis was provided for the displacement scanning transducer. As in the previous arrangement the specimen was rotated past a fixed transducer with angular position sensed photoelectrically.

The result of this operation is a set of displacements representing the radial distance of the shell wall from the axis of rotation.

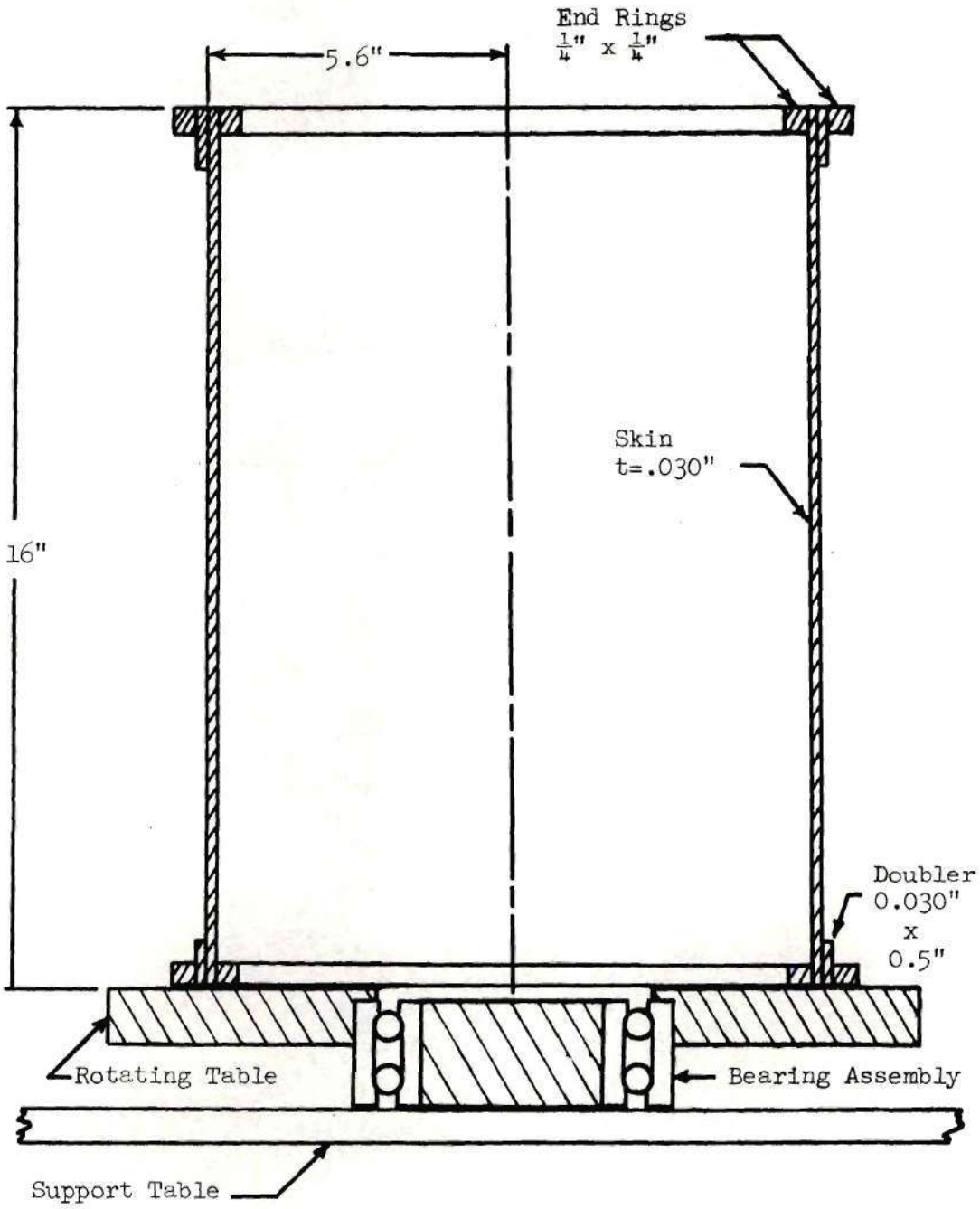

Figure 5. Monocoque Cylindrical Shell Cross-Section and Rotating Table Assembly for Small Specimen Scan.

Eccentricity due to the mounting arrangement can be removed from the measurements leaving the distortion and eccentricity inherent to the shell. These imperfections are represented as before with reference to an ideal or "perfect" cylinder which in a least square sense "best fits" the real shell.

The initial shape of the small scale specimen is displayed graphically in Figure 6. The presentation is similar to that for the large shell (Figure 4). The seam area can be immediately identified as the region of large radius and relatively severe distortion. Its single occurrence in this one panel type construction leaves an apparently greater area of the shell unaffected by its presence than is the case with the six panel construction employed in the full sized shell. A closer examination of this data and analysis of its implications will be reported in Chapter III.

Comparison of Full and Small Scale Specimens

The investigation of the initial geometry for the full and small scale shells must be placed in proper perspective. A comparison of quality can be made on the basis of the standard deviations computed from the refined radial measurement data. Detailed results of this investigation are presented in Table 1. It can be observed that the presence of a single seam in the small scale specimen is more detremental to the results than is the presence of multiple seams in the larger shell. A more representative measure of standard deviation can be obtained for the small scale specimen by ignoring the data in the immediate vicinity of the seam. This yields results which compare

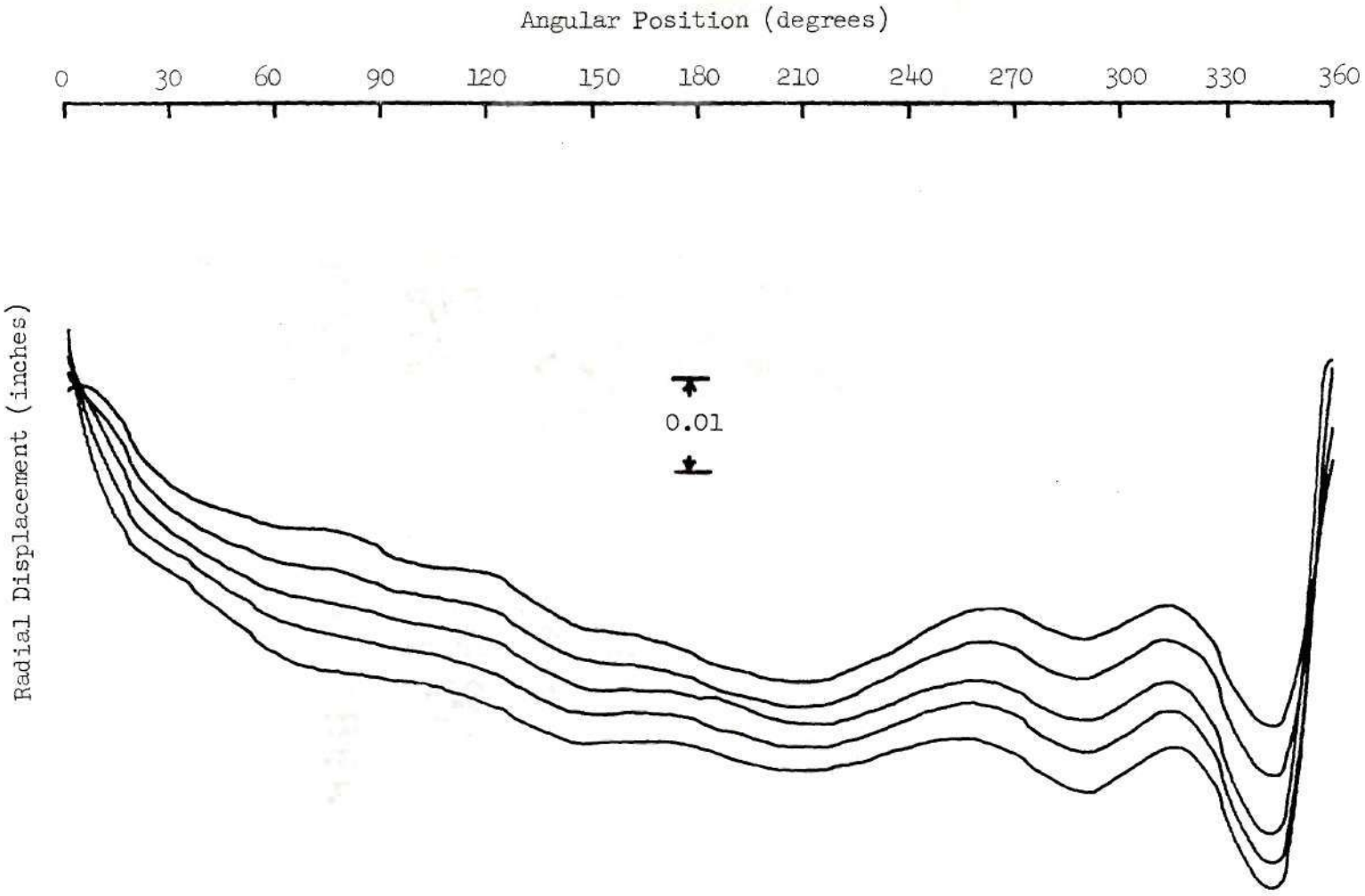

Figure 6. Small Shell Initial Geometry.

Table 1. Normalized Standard Deviations of Radial Measurements for Large and Small Specimens

Position	Small Shell (complete)	Small Shell (omit seam)	Large Shell
Equal Increments Along Shell Axis From End to End	.00836	.00791	.00434
	.00853	.00731	.00740
	.00856	.00673	.00940
	.00904	.00663	.01080
	.00931	.00627	.01215
	.00989	.00604	.01283
	.01134	.00607	.01305
	.01147	.00609	.01302
	.01185	.00613	.01261
	.01265	.00626	.01178
	.01290	.00662	.01065
	.01262	.00709	.00905
	.01266	.00727	.00716
	.01222	.00811	.00571
Average	.01080	.00675	.01050

favorably to the large shell in a quality sense.

A second comparison of specimen quality can be made on the basis of spectral analysis. Initial distortions can be represented by one or two dimensional Fourier series and the series coefficients taken as a spectral estimate. For the present application, the radial distortion along a circumferential generator were represented by a Fourier series over the angular interval zero to 2π. The spectra so generated for each shell are shown in Figure 7. Wavelengths predominant in each specimen can thus be easily identified and their effects analyzed. The second harmonic would be expected to predominate in the small shell and a study of the spectrum confirms this. Similarly, the sixth coefficient is manifested in the spectrum for the large specimen. In both cases the seam influence is the cause. The effects of this, on the other hand, might be considerably different. Analysis and experiment (10) indicate that a circular cylinder would be expected to buckle with wavelengths of from 1/4 to 1/9 of the circumference. Clearly, the small scale shell is not obviously influenced in this spectral region, but the large specimen might be greatly affected by its predominant sixth mode.

The final criterion for comparison of the specimens is purely qualitative. Pointwise determination of lateral wall stiffness is a major aim of this study and the effect of the shell seams can become a significant element of such measurements. A seam area would be expected to separate influences which might otherwise be pronounced. The seam stiffness discontinuity would attenuate the cross coupling of regions on opposite sides of the seam.

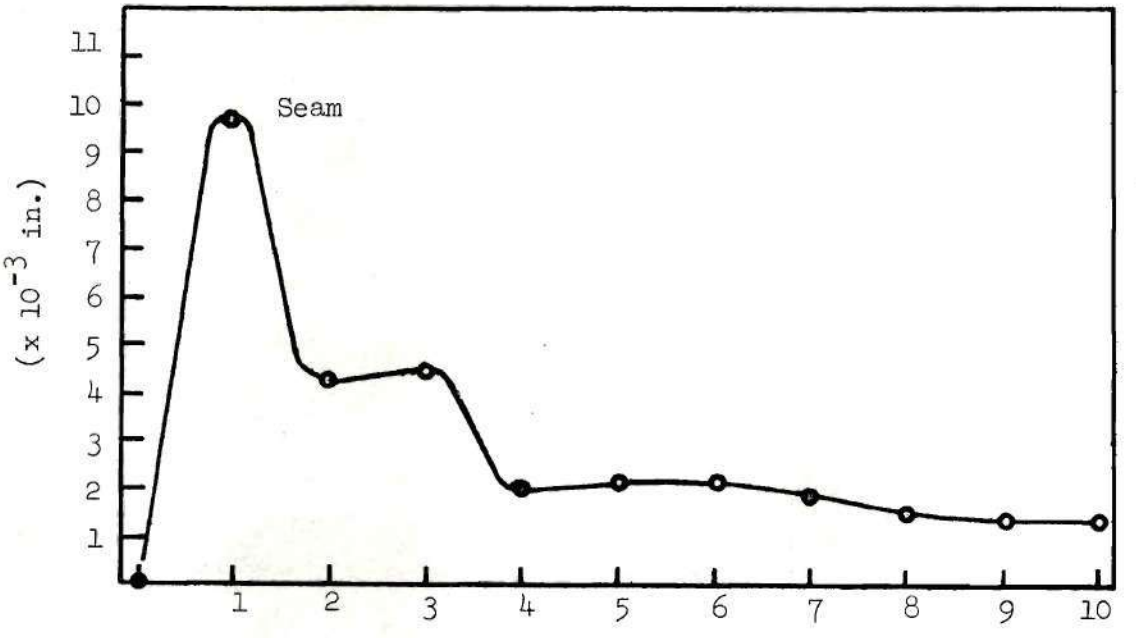

Small Shell

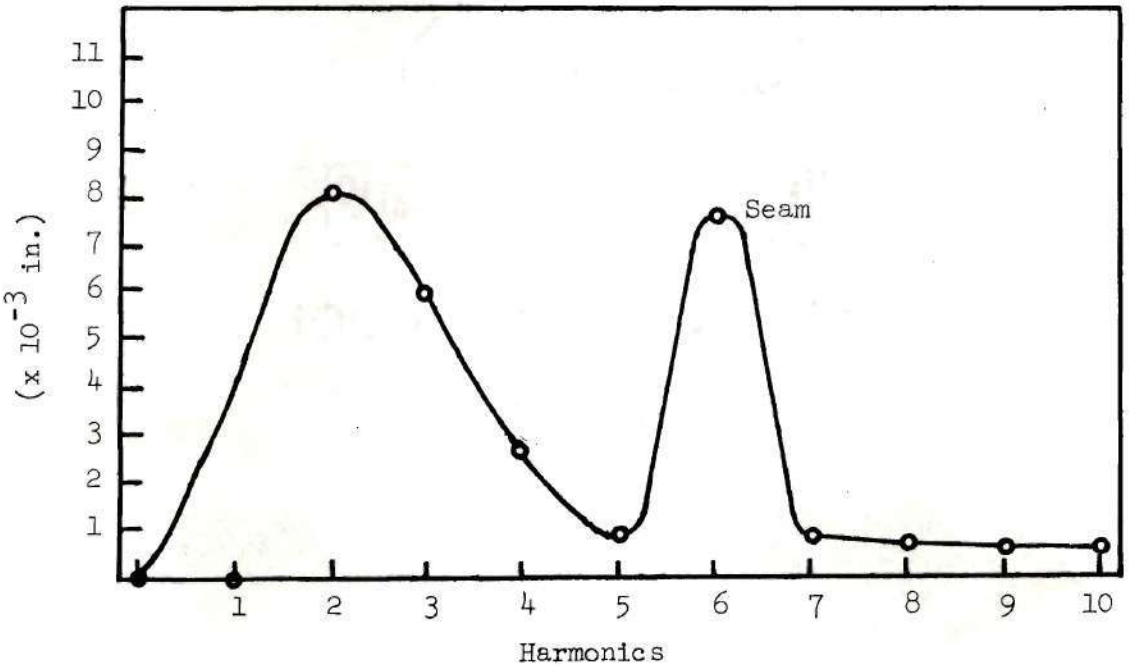

Large Shell

Figure 7. Spectral Analysis of Large and Small Specimens.

With this comparison between the full and small scale vehicles, it becomes evident that for purposes of a preliminary study of structural stiffness and its relation to stability limits the small scale shells are to be preferred. The construction procedure for these models yields specimens with fewer stiffness anomalies. Furthermore the overall geometric quality, as far as has been determined, appears almost equal. For these reasons the stiffness analysis program reported in the following chapters has been restricted to the small scale specimens.

CHAPTER III

ANALYSIS OF CONSTITUTIVE FORM

In the study of structural stability the stress and deformation are generally the points of major interest. The goal of an analytical treatment is to determine a critical value of applied stress above which the structure no longer remains capable of usefully supporting load. From an experimental point of view the goal is to identify the precise mechanisms responsible for the behavior. Major effort in experimental work has been to identify characteristic patterns of load behavior (stress reversal for instance) or predictable patterns of distortion. In connection with the latter point it has, in recent times, become popular to employ the "Southwell Plot" procedure to extrapolate from deflection data the critical value of loading. This procedure has proven quite powerful for a broad variety of problems for which the distortion behaves hyperbolically with loading. The most serious drawbacks to this procedure have been twofold:

1. For some cases the distortion must be measured only at certain points (usually unknown in practice).

2. Useable data is sometimes obtained only at relatively high levels of destabilizing load (especially if the level of imperfection is low).

It is largely for these reasons that direct application of the procedure to stability problems involving cylindrical shells under axial

load has been notably unsuccessful.

Structural Stiffness

Deflection and stress measurements by themselves are not the only means by which to interpret experimental tests. Stiffness of the structure affords an attractive alternative measure and, in fact, incorporates both the stress and deformation in its definition.

Structural stiffness is, of course, a familiar engineering concept. Its precise meaning may vary from one application to another however. In a strict sense stiffness is an attribute only of a linear material or structure. When a force is applied to a linearly elastic material, a proportional deflection is produced. The stiffness is defined directly as the measure of proportionality - force per unit deflection - while the flexibility is defined as the stiffness reciprocal. Stiffness (or flexibility) influence coefficients are then defined as the proportionality factors between a force acting at one material point and a deflection at another.

Nonlinear Stiffness

Deflection due to loading is not always linear over the complete range of interest for many linearly elastic structural problems. The column lateral deflection becomes noticeably hyperbolic under the influence of lateral loading. If one attempts to speak of lateral stiffness for this problem, the domain of deflection must be specified. Since stiffness is a linear concept, then a unique value of the quantity cannot be determined which is applicable to the entire range of force and corresponding deflections. A possible alternative is a definition of stiffness based upon incremental values of force and deflection.

The later case is most easily accomplished and is the approach taken in this work.

Two approximations to lateral stiffness are employed and their definitions follow:

1. Quiescent Stiffness - The lateral stiffness of the shell wall at zero lateral test force. This value is extrapolated from data taken at low values of lateral force.

2. Differential Stiffness - The lateral wall stiffness calculated incrementally at large values of lateral test forces and deflections.

The quiescent stiffness is shown approximated by the slope of the solid line joining points 1 and 2 on Figure 8. The slope of the dashed line between points 8 and 9 is the equivalent approximation to the differential stiffness.

Stiffness and Stability

The behavior of structural stiffness in a stability study must first by understood before a useful application of the concept can be attempted. It can be demonstrated through classical analysis that the lateral stiffness of a structure decreases to zero under the action of a destabilizing load. This, of course, is a situation unique to problems of structural stability and can be explained by considering the beam column. At values of axial load less than critical, any lateral force produces a corresponding unique deflection of the same order of magnitude. At the critical axial load (Euler load), however, an infinitesimal lateral force produces a deflection which is arbitrary. At this load, then, an infinitesimal force and a finite deflection give

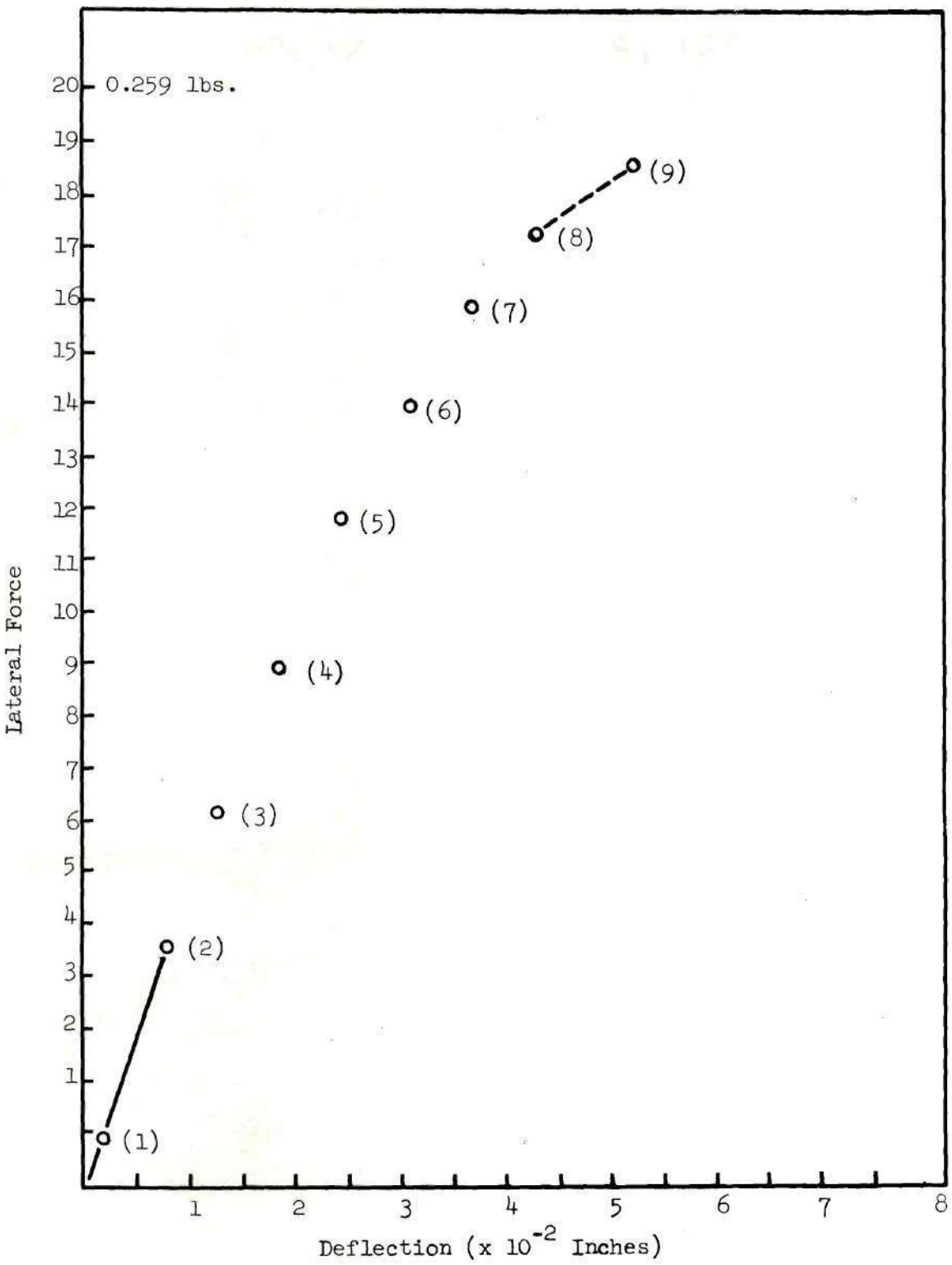

Figure 8. Typical Lateral Force - Deflection Data.

rise to a lateral stiffness of zero. An analysis is presented in the following section which demonstrates the lateral stiffness - stability characteristics of simple structures.

Simple Structural Models

Insight can be gained in the topic of structural stiffness if simple models are employed in an analysis of load and deflection. The results obtained are particular cases, but point out the generality of the underlying idea.

The Column

The uniform straight pin ended column was considered by Bank (9) and he pointed out that if w, the lateral displacement at the center of the column is expressed as a function of the applied concentrated lateral load, Q, then the relationship between load and deflection can be approximated by the expression

$$w = \frac{QL^3}{48EI}\left[\frac{1}{1 - \frac{P}{P_{cr}}}\right]$$

If lateral stiffness is defined as the ratio of the lateral load to the resulting deflection, the result above can be expressed as

$$K_L = \frac{Q}{w} = \frac{48EI}{L^3}\left[1 - \frac{P}{P_{cr}}\right]$$

Clearly, the approach of the axial load to its critical value results in a stiffness decrease toward zero. It may also be seen that the approximate relationship is linear.

The Flat Plate

Turning now to the simply supported flat plate with uniform inplane compression in one direction (x) and loaded laterally by a concentrated point force at the center, the central deflection can be expressed as follows.

$$w = \frac{4Q}{ab\pi^4 D} \sum_{m=1}^{\infty} \sum_{n=1}^{\infty} \frac{1}{\left(\frac{m^2}{a^2} + \frac{n^2}{b^2}\right)^2 - \frac{m^2 N_x}{\pi^2 a^2 D}} \sin \frac{m\pi x}{a} \sin \frac{n\pi y}{b}$$

Defining $N_{x_{mn}}$ as the mn^{th} critical load,

$$N_{x_{mn}} = \left[\frac{m^2}{a^2} + \frac{n^2}{b^2}\right]^2 \frac{\pi^2 a^2 D}{m^2}$$

Then

$$w = \frac{4Q}{ab\pi^4 D} \sum_{m=1}^{\infty} \sum_{n=1}^{\infty} \frac{1}{\left[\frac{m^2}{a^2} + \frac{n^2}{b^2}\right]^2} \frac{\sin \frac{m\pi}{2} \sin \frac{n\pi}{2}}{1 - \frac{N_x}{N_{x_{mn}}}}$$

For inplane compressive loading in the x direction, the n^{th} term is fixed at unity, but the m^{th} term is determined by the ratio of the length of the sides. Considering for simplicity a rectangular plate, $a < \sqrt{2}\, b$, the result is approximately

$$w = \frac{4Qa^2}{\pi^4 D\left(\frac{b}{a}\right)\left(1 + \left(\frac{a}{b}\right)^2\right)^2} \quad \frac{1}{1 - \frac{N_x}{N_{x_{11}}}}$$

Thus as for the column, an expression of lateral stiffness is derived.

$$K_L = \frac{Q}{w} = \frac{\pi^4 D}{a^2}\left(\frac{b}{a}\right)\left(1 + \frac{a^2}{b^2}\right)^2\left(1 - \frac{N_x}{N_{x_{11}}}\right)$$

Clearly for the flat plate, as for the column, lateral stiffness is approximately a linearly decreasing function of compressive load.

Cylindrical Shells

The column and plate have been shown to respond hyperbolically under the influence of lateral force cum compression. Since similar behavior is well known to be evident without lateral disturbance (2,3), one can surmise that the results are complimentary.

Flügge (11) has demonstrated analytically, but with some reservation, that the Southwell method applies to the cylindrical shell under axial compression. The assumption can this be made that,

like the column and plate, a hyperbolic deflection response is present due to lateral force coupled with compressive loading. The analysis problem is not to be treated in this predominately experimental thesis, but the assumption has been confirmed through experiment by Bank (9).

CHAPTER IV

EXPERIMENTAL STUDY OF LATERAL STIFFNESS

Lateral Stiffness Measurement Apparatus

Lateral stiffness of the specimen was studied by means of the apparatus depicted schematically in Figure 9. The primary function of the assembly was to apply a continuously adjustable and measured point force normal to the shell wall and to determine the resulting deflection at the point of application. A small blunt probe was afixed to a traverse table and positioned so that when the table was advanced by a micrometer head, the probe pressed against the shell wall. The load transmitted to the specimen was detected by a sensitive load transducer (employing an LVDT as the sense element) to which the probe was mounted. Motion of the traverse table relative to the shell axis was detected by an LVDT displacement transducer as shown. The output from this transducer should represent the forcing point deflection and thus be used directly to compute stiffness. However, the load transducer had a compliance of the same order of magnitude as the shell itself, and thus, there was a finite relative displacement across the load transducer that had to be accounted for in determining the forcing point deflection. The load transducer compliance was constant and so deflection across it could be linearly related to applied load. The output of this transducer, then, represented both a load and a unique deflection of the transducer itself.

It is clearly evident that if d_1 is the deflection across the load transducer and d_2 is the motion of the traverse table, then the deflection of the shell wall is given as

$$\alpha = d_2 - d_1.$$

An analog scaling and computing circuit using a combination of operational amplifiers was used to electrically calculate the deflection, α, and to normalize the load output. The circuit is shown in Figure 10. Output voltages proportional to α and Q, the lateral point force, were fed to an HP 7004A X-Y recorder and then plotted in cartesian form. From these plots appropriate stiffnesses could be directly computed.

Stiffness Reduction

Continuous plots of lateral force versus resultant lateral deflection were the desired output of the measuring apparatus. Difficulty in obtaining these curves was encountered due to the extreme sensitivity of the equipment to slight disturbing influences present during normal operation. This necessitated a compromise solution be adopted. A given level of lateral force was applied to the shell wall and sufficient settling time allowed for decay of extraneous disturbances. The lateral force and displacement were then recorded as a discrete point. Figure 8 is a typical data plot resulting from this procedure.

If lateral stiffness is calculated based upon the deflections

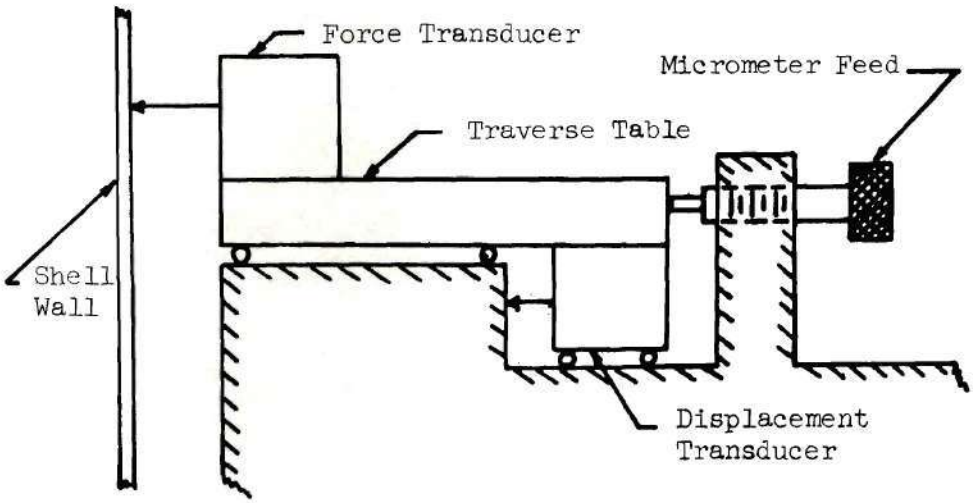

Figure 9. Force - Deflection Measurement Device.

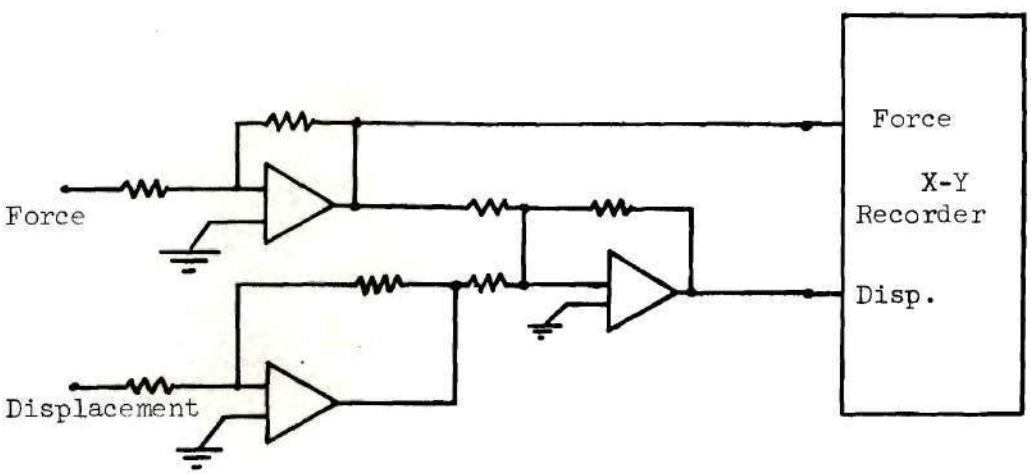

Figure 10. Force - Displacement Signal Conditioning and Plotting Circuit.

resulting from incremental lateral test forces, then any nonlinearity of the data would result in distinct combinations of lateral force levels and corresponding lateral stiffnesses. This multiple force method is preferred in this analysis because of the freedom allowed the experimentalist in choosing the deflection region to be investigated, whether it be linear or nonlinear.

Investigation of Monocoque Shell

The experimental program of stability investigation of the specimen was performed in two sequential parts. A zero axial load lateral stiffness survey of the complete specimen was performed in an attempt to correlate initial geometry with initial stiffness. Possible critical areas, as determined from these studies, were then investigated with the shell under axial compression.

Initial Stiffness Investigation

The specimen, under zero axial compression, was initially probed on a coarse grid spacing of 30 degrees circumferentially and $2\frac{1}{2}$ inches axially. The results, as expected, showed that the central portion of the shell was consistently lower in lateral stiffness than those points approaching the ends. Thus this central area was investigated on a finer grid spacing of $7\frac{1}{2}$ degrees, resulting in 47 points of initial stiffness data (the seam was not probed).

The quiescent stiffnesses, as defined in Chapter III, are shown plotted in Figure 11. A three point interpolation scheme was applied to these points to more clearly identify areas of relative minimum and maximum stiffness, as shown in Figure 12.

A second measure of lateral stiffness was also evaluated: the aforementioned differential stiffness. Although the lateral stiffness magnitudes are necessarily diminished because of the nonlinearity, a great similarity is apparent in these results (Figure 13) and those of the interpolated data. It is suggested that the higher levels of lateral force are reacted by an increases surface area, an interaction which would tend to produce an averaging effect of neighboring regions, the result being an effectively smoother stiffness picture.

Initial Geometry Correlation

The initial geometry contours of Figure 6 show three areas with a relative low or flattened region. These segments can be identified in the following locations: 160 - 240 degrees, 255 - 315 degrees and 320 - 350 degrees. All correspond to regions of relative minimum stiffness and are promising points at which to investigate stiffness decrease under axial load.

The seam of the shell would be expected to increase the stiffness, as is shown in the data, and the plots indicate that for this particular specimen the region affected is approximately 60 degrees to either side of the seam. Therefore, two of the relatively flat areas are likely to be influenced by their proximity to the seam. The remaining area, from 160 to 240 degrees, is most likely to show a relationship between the stiffness decrease under axial load and the relative minimum stiffness of the zero axial load data previously obtained. It is noted also that the wave length of the imperfection in this region is greatest, a factor found relevant in the prediction of regions of instability by Horton and Craig (12).

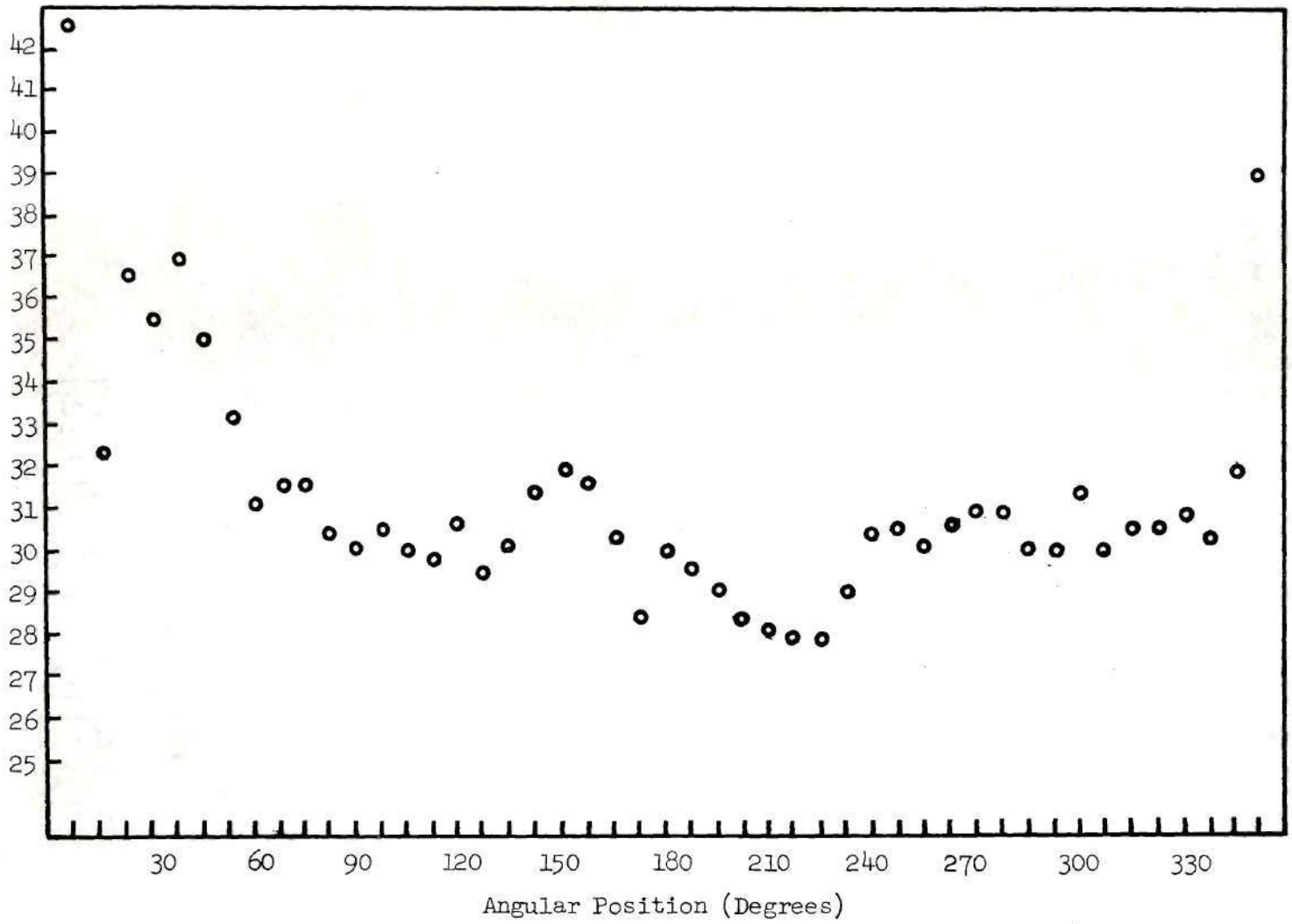

Figure 11. Quiescent Stiffness of Monocoque Shell.

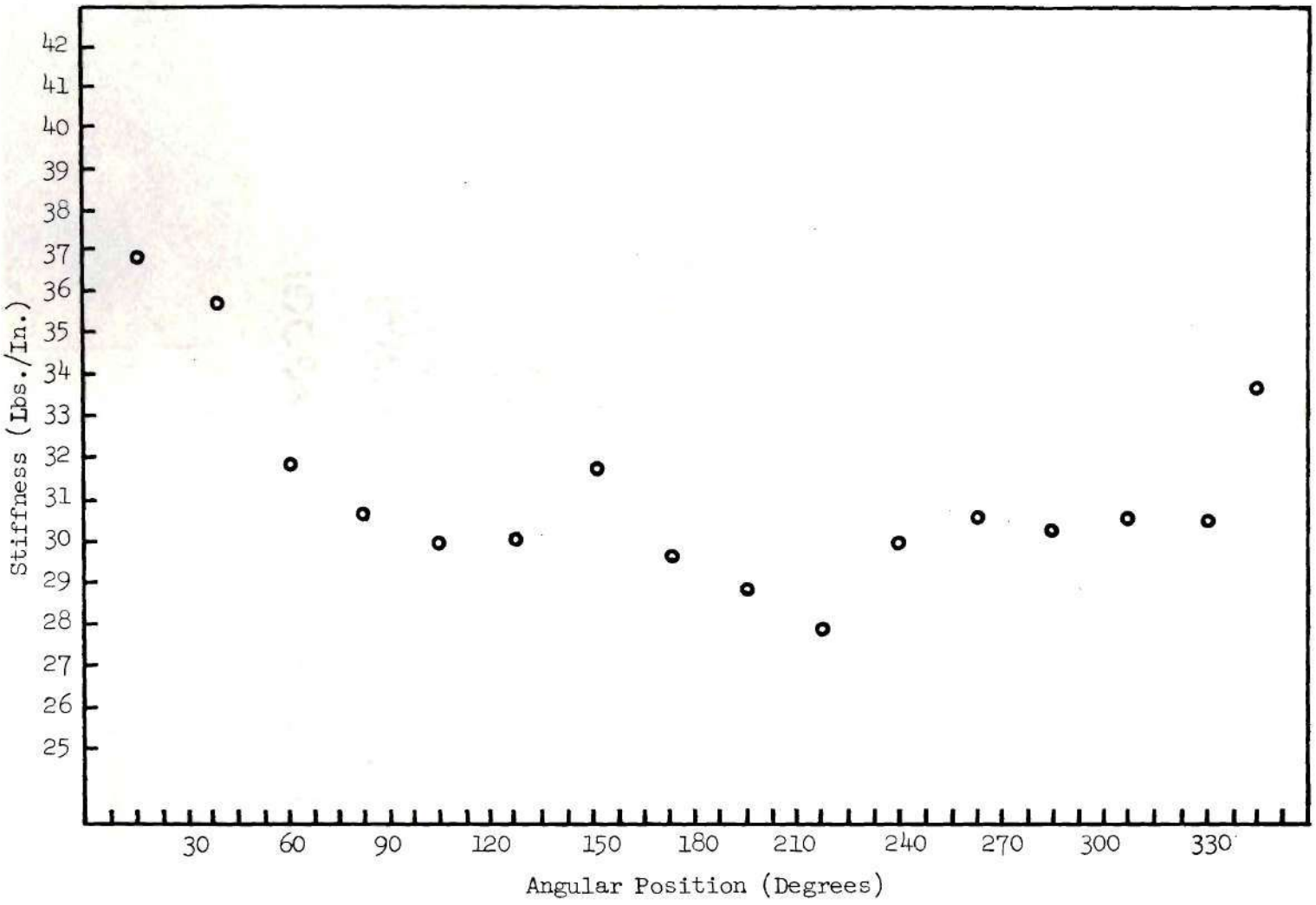

Figure 12. Interpolated Quiescent Stiffness of Monocoque Shell.

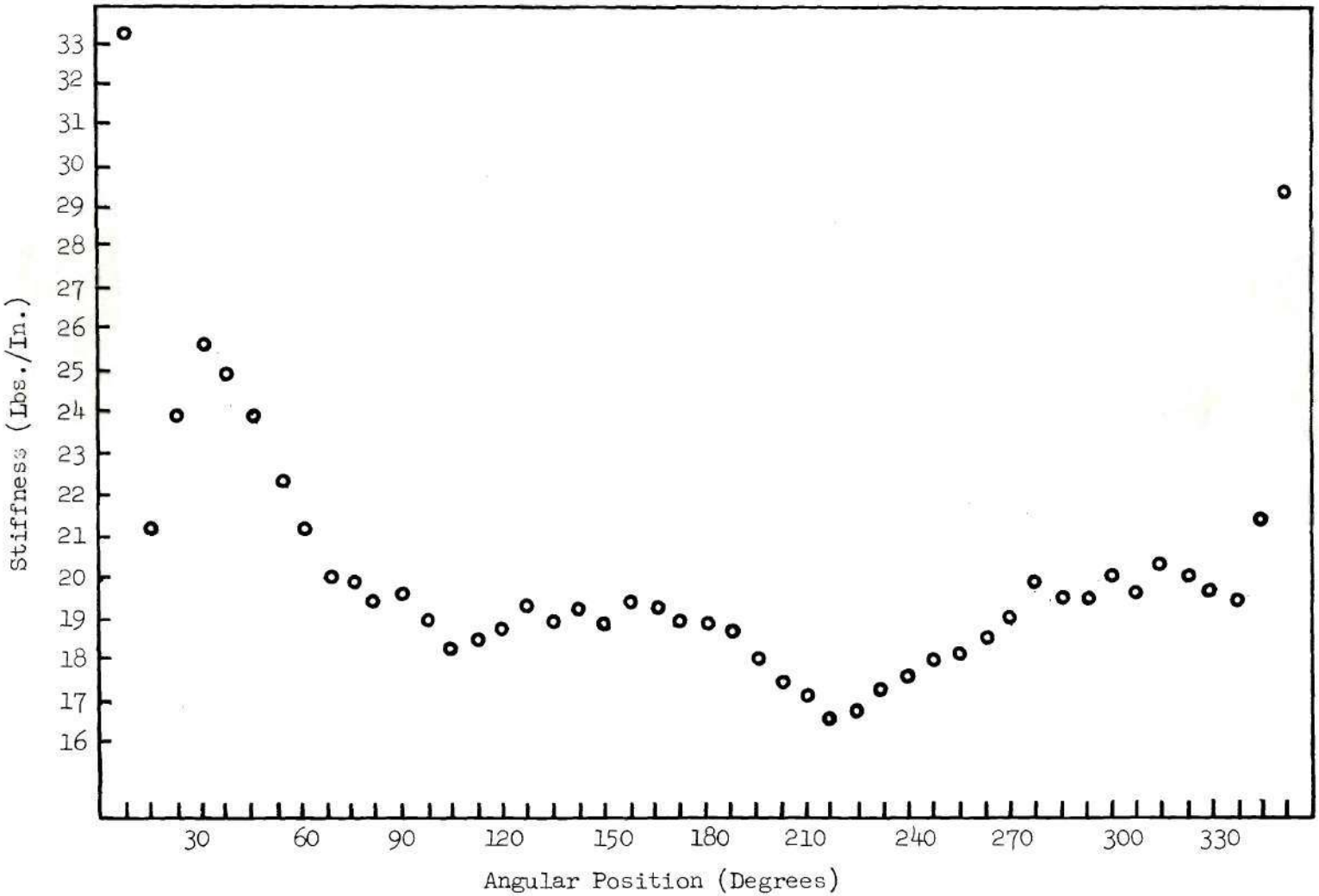

Figure 13. Differential Stiffness of Monocoque Shell.

Instantaneous Stiffness Decrease Under Axial Load

The point of minimum lateral stiffness is clearly seen to be the 220 degree position. It was this point, then, which was concentrated upon in the subsequent investigation.

Bank (9) found that for a stiffened cylindrical shell loaded by a discrete lateral point force, the lateral stiffness was a decreasing function of axial compressive load. Further, this decrease was linear and could be extrapolated to zero at the experimentally determined critical compressive load. In an attempt to investigate the unstiffened shell in a similar fashion, the quiescent stiffness was determined for several values of lateral load. The results of this investigation are tabulated in Table 2. These stiffnesses are also plotted as a function of axial load in Figure 14. It is evident that if the critical compressive load were determined by extrapolating the stiffnesses calculated below 500 pounds axial load, the apparent buckling load would be above 2000 pounds. This is approximately 140 per cent of the classically determined instability value.

At higher compressive loads, from 730 to 750 pounds, a break is observed in the stiffness plot and the rate of decrease is observed to be much more rapid. An extrapolation of these points results in a buckling load of about 940 pounds, or approximately 70 per cent of the classical value. It is also significant that this result is achieved above 75 per cent of the experimentally determined critical load.

Southwell Investigation of Force-Deflection Data

To this point the lateral force-deflection data has been investigated solely upon the basis of interpretation of lateral

Table 2. Quiescent Stiffness Decrease Under Axial Load

Axial Load (lbs.)	Instantaneous Stiffness (lbs./in.)
40	26.524
160	24.812
220	24.419
250	22.961
280	22.513
400	22.295
440	21.667
480	21.366
520	20.512
730	17.415
740	16.721
750	15.859

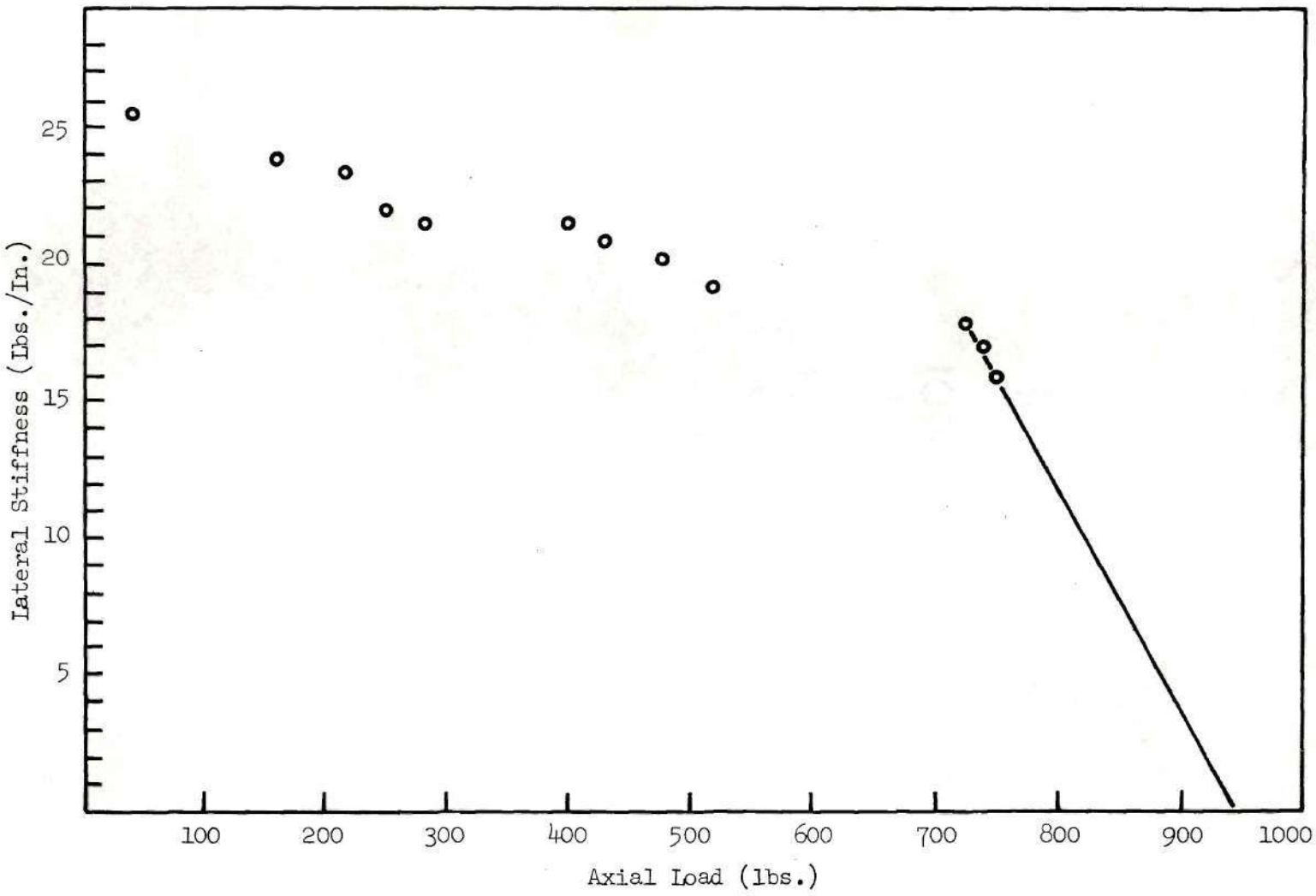

Figure 14. Instantaneous Stiffness Behavior Under Axial Load.

stiffness. The characteristic nonlinearity has been observed, but not explained. Observation of the data reveals that deflection increases not only disproportionately with lateral load, but also in a manner indicating a weakening of the structure with increased side force. This is a characteristic common also to the arch and curved panel approaching a snap-through instability due to lateral loading. The question to be answered now is whether this snap-through load can be identified, and if so, then what is its behavior under increased axial load.

Figure 15 is representative of the data obtained at the 220 degree position. It can be seen that under increased axial load, the nonlinearity of the data is enhanced. In an attempt to identify the critical lateral force loads for the data, the Southwell process was applied to the information. Although the technique was first applied to the column, it is based upon the principle that any rectangular hyperbola can be represented as a straight line under a proper change of coordinates.

In this investigation, force and deflection need not be known in an absolute sense. The data is considered plotted relative to equally incremented ordinate and abscissa and thus the horizontal asymptote determined in the Southwell analysis is expressed in these arbitrary units. The actual critical force is easily found by scaling these units against the known force calibration.

The curves of Figure 15 for three axial force levels are shown plotted in Southwell form in Figure 16. The deviations of the lower points are to be expected. This is an indication of measurement

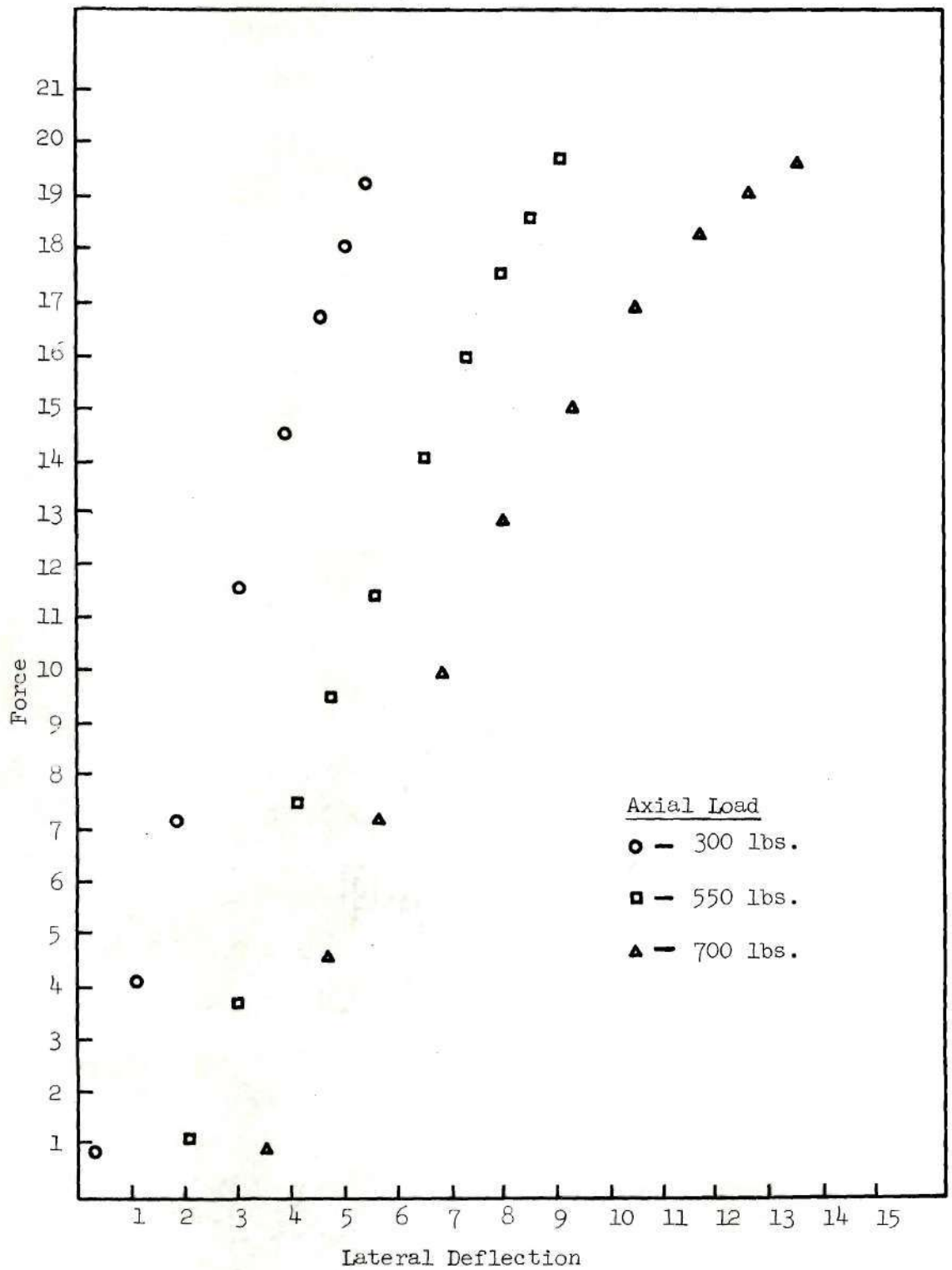

Figure 15. Load - Deflection Plots, Increasing Axial Load, for 220 Degree Angular Position.

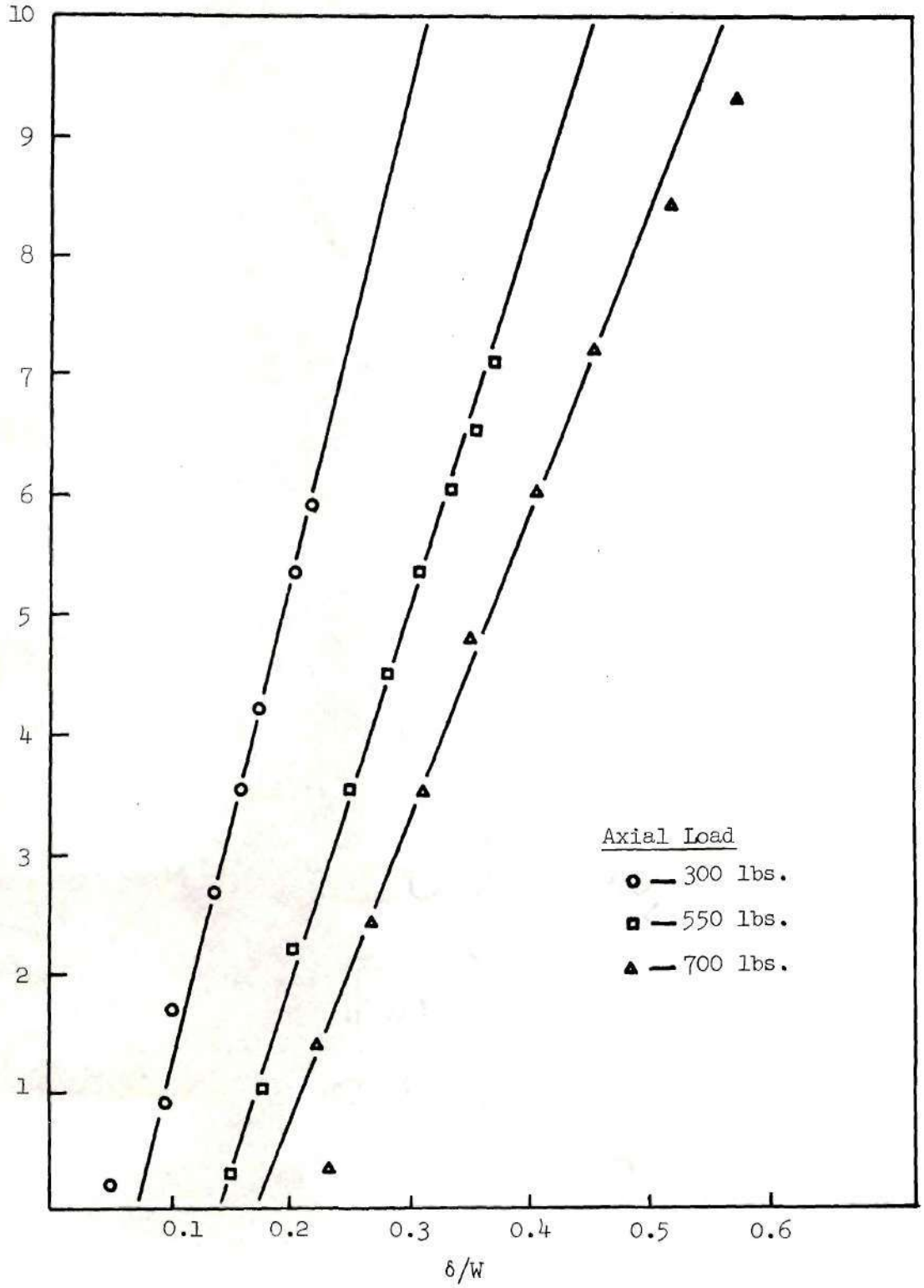

Figure 16. Southwell Plots of Load-Deflection Data.

uncertainty and the nonhyperbolic nature of the low lateral force data points. Also to be anticipated is a region of high lateral force levels in which the deflections are again non-hyperbolic. The simplifying assumption of negligible midplane stretching is no longer valid for these lateral force ranges. The deformed surface cannot be considered a "developable" one, and thus the associated deflections are significantly influenced by the nonlinearities associated with this midplane strain. The result is the observed derivation from linearity in the Southwell procedure. A complete summary of axial load and critical side force is presented in Table 3.

The question to be answered now is what significance can be given to these critical lateral loads in the investigation of compressive stability. The answer is quite apparent in Figure 17, a plot of critical lateral load as a function of axial compression of the specimen. The extrapolation of the data to a buckling load of 940 pounds (the same as was determined by the quiescent stiffness investigation) is undeniable.

All of the above compression studies were performed with a Baldwin test machine of the constant end shortening screwjack type. As a test of the accuracy of the above results, the specimen was compressed until buckling occurred. The observed critical load was 942 pounds.

Table 3. Critical Lateral Forces as Determined by Southwell Method

Axial Force (lbs.)	Maximum Lateral Load (lbs.)	Critical Lateral Load (lbs.)
50	0.690	3.880
100	0.690	2.743
200	0.690	2.000
300	0.690	1.710
400	0.690	1.465
450	0.259	1.337
500	0.259	1.218
550	0.259	1.050
600	0.259	0.932
650	0.259	0.750
700	0.259	0.647
720	0.259	0.596

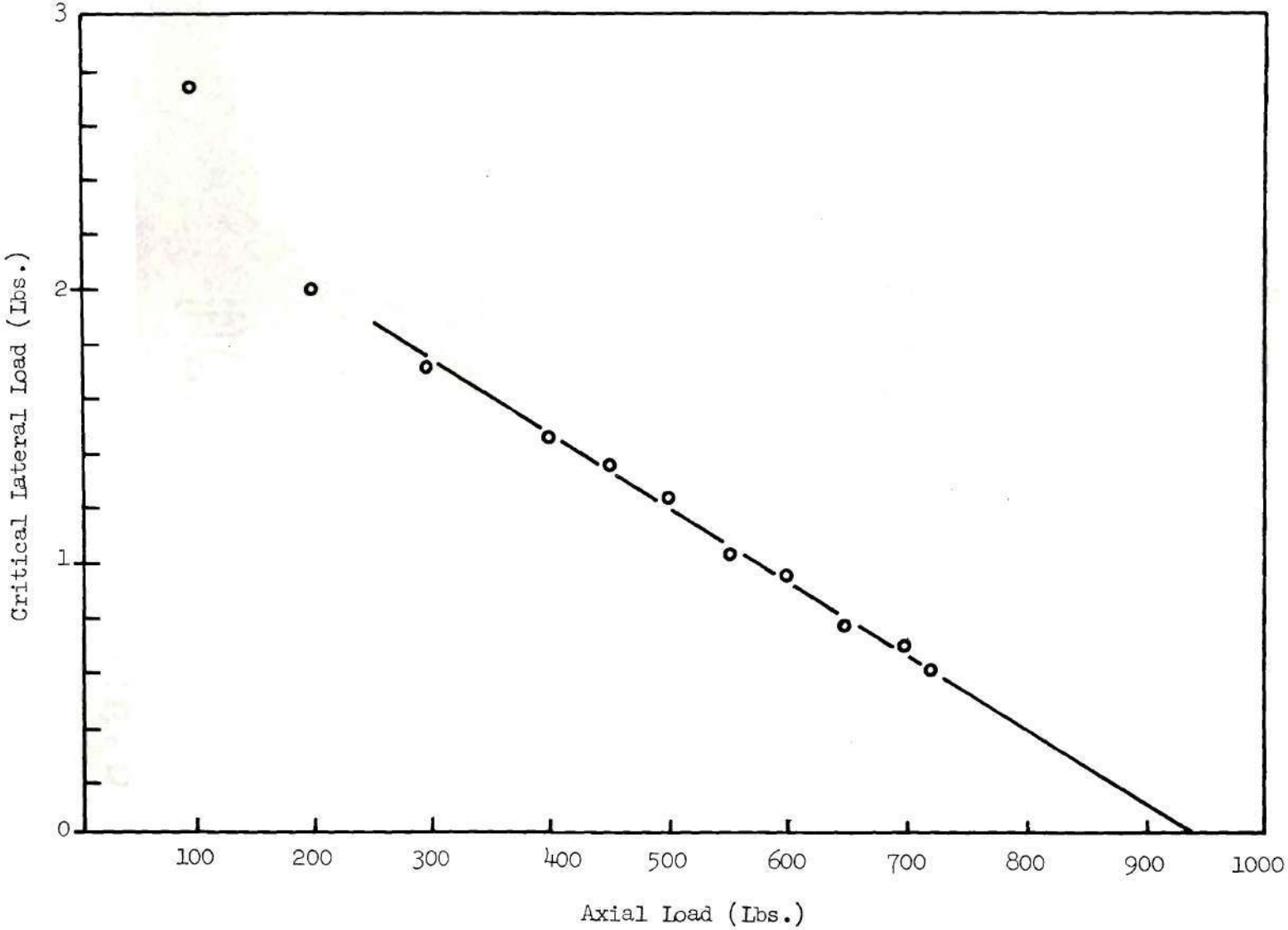

Figure 17. Critical Lateral Force Behavior Under Axial Compression.

CHAPTER V

CONCLUSIONS

Two goals were reached in the research undertaken for this thesis; a comparison of initial geometry with initial lateral stiffness was made, and an extension of Bank's (9) nondestructive test procedure for determining critical compressive loads of circular cylindrical shells was developed. The comparison of initial stiffness and geometry strongly indicated that initial stiffness is directly related to the degree of curvature present in localized areas of the specimen. Further, the point of lowest stiffness at zero axial load was found to be an area suitable for axial compression studies in the prediction of buckling loads.

Two methods were found accurate in the prediction of critical load for the monocoque shell, the first of which was the procedure introduced by Bank. However, a shortcoming was observed in this method. When the quiescent stiffness (approximated by low lateral test forces) was investigated under axial load, accurate prediction was obtained only at a compressive load range above 60 per cent of the buckling value. Other approximations to the stiffness (such as those determined at high values of lateral test force) might lower this prediction interval, and further study in this area is warranted.

This stiffness criterion is fully equivalent in formulation to the well established Southwell plot procedure. As Fisher (13) pointed

out, the presence of lateral loading can be considered as an imperfection which does not alter the critical load but does augment the effective level of geometric imperfection. The utility of the present stiffness formulation rests with this later point. A direct application of the Southwell plot to high quality structures (i.e., low imperfection level) usually proves difficult because the characteristic asymptotic behavior of load and deflection does not become pronounced until loading is almost to its critical value. Furthermore, in many shell structures the hyperbolic behavior can be observed only at selected (and generally unknown) points on the surface. These problems can be partially offset by applying lateral forces so as to increase the imperfection and render the behavior more apparent at lower load levels. This is effectively accomplished in the application of the lateral stiffness criterion. Similar benefits should be obtained by direct application of the Southwell plot if a constant point lateral load is also acting. This later technique has not been actively pursued here because of practical difficulties in its implementation.

A second method for investigation of critical load levels was introduced, and similarly, yielded accurate predictions for the critical loads. The technique is not related to the direct Southwell plot procedure although that method is used indirectly in determining critical load predictions. The differences in the two methods are masked by the similarities of the investigative technique used. Both employ lateral static loading as a test mechanism but, of course, one must recall that lateral stiffness can be measured in several ways, including a dynamic approach as indicated earlier.

The procedure now introduced is to use an imperfection insensitive but destabilizing force in the study of a more violently destructive loading which is imperfection sensitive. The test loading employed for these tests on cylindrical shells was a point force acting normal to the shell wall. Load-deflection data from this loading was analyzed (via the Southwell plot) for different levels of applied axial compression. The result of this is an interaction relationship similar, for instance, to what might be obtained from a coupled compression - torsion loading. Strikingly different, however, is the order of the interaction curve obtained in the lateral test force study. The results have shown the curve to be approximately linear and therefore it is possible to extrapolate the data to an accurate prediction of critical load under pure axial compression. This particular interpretation is, of course, valid only for the present combination of destabilizing loading, but other extrapolation schemes (nonlinear, perhaps) can be developed for other structural elements and combination loadings. For example, the present method clearly would not work for a simple column because the test force does not create a destabilizing load.

This preliminary investigation has shown that accurate prediction of critical axial load can be obtained at a small fraction of the buckling load. A decrease of approximately 50 per cent below the prediction range of the quiescent stiffness procedure was observed. A drawback is realized, however, when one considers the labor necessary to calculate even a single data value by this more involved technique. A compromise is indicated in the use of both procedures for this type

of stability investigation.

Although a test upon a single specimen is seldom considered conclusive, the accuracy of both experimental methods cannot be overlooked. In both cases, the error was found to be less than 1 per cent of the predicted value. It was clearly demonstrated that the stability investigation should be conducted at the point of lowest initial stiffness. Experimental work is continuing in these areas, and even more encouraging results are expected.

APPENDIX

DATA AQUISITION AND FLOW DIAGRAM

The circularity measure of the cylindrical specimens was computed from the radial displacement data acquired using the following BASIC language program. Data and control logic was as shown in figure 18.

```
1   DIM V[1],A[185]
2   GOSUB 700
3   LET N=1
4   GOSUB 400
5   LET I=5
6   PRINT
7   GOSUB 300
10   CALL (2,15,S)
11   IF S<0 THEN 999
12   CALL (2,0,S)
13   IF S>0 THEN 10
15   LET I=I+1
20   GOSUB 600
30   CALL (1,X,96)
35   LET A[I]=X/C+D
40   IF I=185 THEN 200
45   GOSUB 625
50   GOSUB 600
60   GOSUB 625
70   GOTO 15
200   PRINT "DATA TAKEN"
202   CALL (2,13,S)
205   IF S<0 THEN 260
210   CALL (2,14,S)
215   IF S>0 THEN 202
220   CALL (11,A[1],T,185)
225   IF T#0 THEN 250
227   PRINT "DATA WRITTEN"
228   LET N=N+1
230   CALL (2,0,S)
235   IF S<0 THEN 230
240   GOTO 5
250   PRINT "WRITE: S=";T
```

```
255  GOTO 5
260  PRINT "NO DATA KEPT"
265  GOTO 5
300  PRINT "BAY, POS.";
305  INPUT H1,H2
310  PRINT "RECORD";R0+N-1
320  LET A[1]=R0+N-1
321  LET A[2]=H1
322  LET A[3]=H2
323  LET A[4]=1
324  LET A[5]=0
330  RETURN
400  PRINT "STARTING REC.";
405  INPUT R0
410  CALL (10,0,T)
415  FOR J=1 TO R0-1
420  CALL (10,1,T)
425  IF T#0 THEN 435
427  NEXT J
430  RETURN
435  PRINT "10:  S=";T
440  END
500  PRINT "ABORT!"
505  CALL (2,0,S)
510  IF S<0 THEN 505
515  GOTO 5
600  CALL (7,V[1],0,1,20)
602  CALL (2,1,S)
604  IF S<0 THEN 500
606  IF V[1]>-250 THEN 600
608  RETURN
625  CALL (7,V[1],0,1,20)
627  CALL (2,1,S)
629  IF S<0 THEN 500
630  IF V[1]<-250 THEN 625
631  RETURN
700  PRINT " REFERENCE RADIUS AND LVDT CALIB. ARE";
710  INPUT D,C
720  RETURN
999  END
```

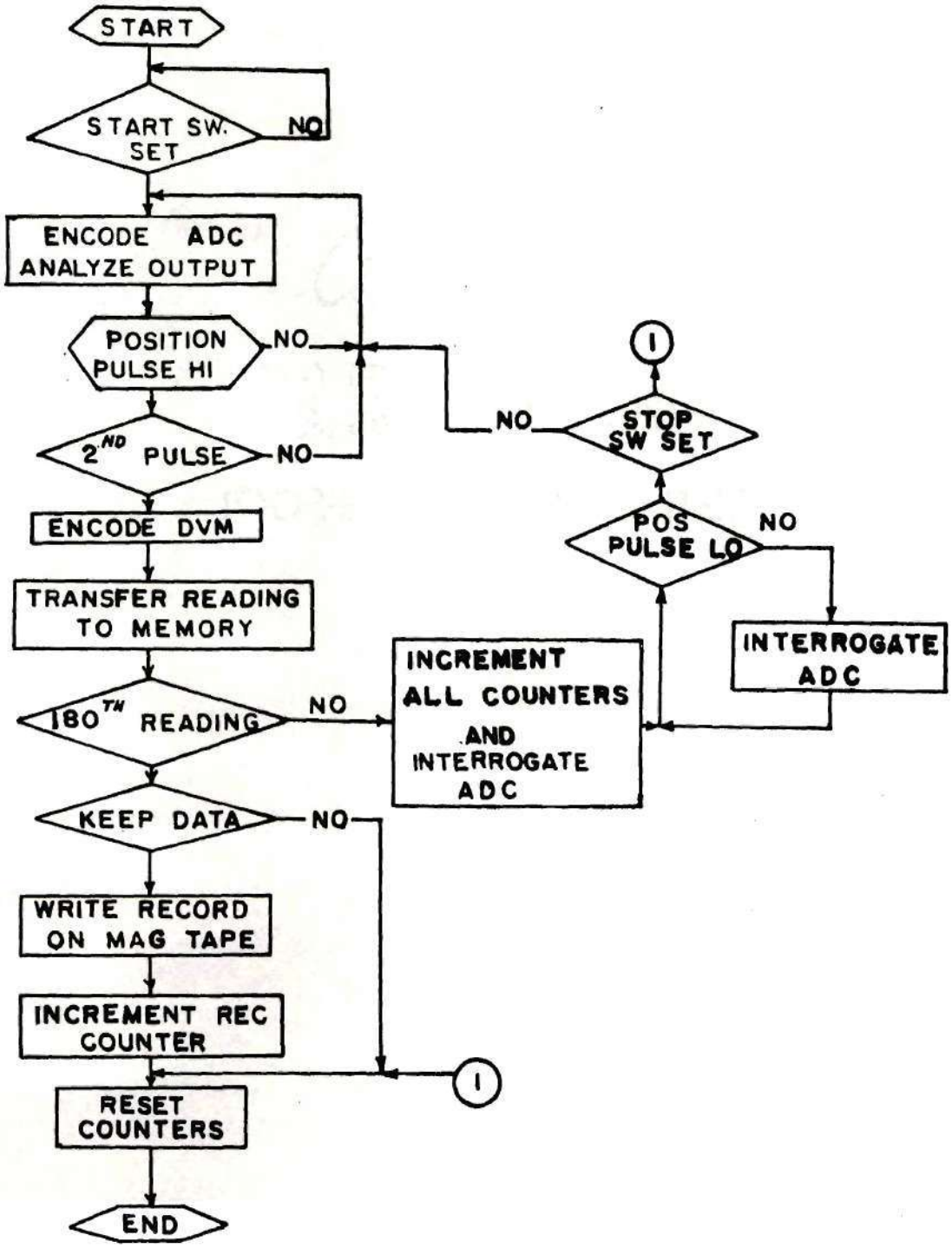

Figure 18. Data Acquisition and Flow Logic of Geometry Analysis Program.

BIBLIOGRAPHY

1. Hoff, N. J., "Thin Shells in Aerospace Structures," Astronautics and Aeronautics, February 1967.

2. Southwell, R. V., "On the Analysis of Experimental Observations in Problems of Elastic Stability," Proceedings of the Royal Society, Vol. 135A, 1932.

3. Horton, W. H., Cundari, F. L. and R. W. Johnson, "The Analysis of Experimental Data Obtained from Stability Studies on Elastic Column and Plate Structures," Israel Journal of Technology, Vol. 5, No. 1-2, 1967, pp. 104-113.

4. Horton, W. H., Craig, J. I., "Experimental Studies of the Effect of General Imperfections on the Elastic Stability of Thin Shells," Israel Journal of Technology, Vol. 7, No. 1-2, 1969, pp. 91-103.

5. Arbocz, J., Babcock, C. D., "Experimental Investigation of the Effect of General Imperfections on the Buckling of Cylindrical Shells," California Institute of Technology, GALCIT Report SM 68-7, 1968.

6. Ford, J. S., "Parametric Studies on the Stability of Stringer and Ring Reinforced Circular Shells," Ph.D. Thesis, Georgia Institute of Technology, Atlanta, Georgia, November 1970.

7. Lurie, H., "Lateral Vibrations as Related to Structural Stability," Journal of Applied Mechanics, 1952, pp. 195.

8. Bolotin, V. V., The Dynamic Stability of Elastic Systems, Holen-Day Inc., San Francisco, 1964.

9. Bank, M. H., "Some Discussions on the Stability of Structural and Mechanical Systems," Ph.D. Thesis, Georgia Institute of Technology, Atlanta, Georgia, August 1971.

10. Komp, R. L., "The Influence of Geometry on the Buckling of Thin Walled Circular Cylindrical Shells," Stanford University, Engineer's Thesis, July 1965.

11. Flugge, W., Stresses in Shells, Springer-Verlag, Berlin, 1960, p. 466.

12. Horton, W. H., Craig, J. I., "Experimental Observations on the Instability of Circular Cylindrical Shells," Israel Journal of Technology, Vol. 6, No. 1-2, 1968, pp. 101-116.

13. Fisher, H. R., "An Extension of Southwell's Method of Analysing Experimental Observations in Problems of Elastic Stability", Proceedings of the Royal Society, Vol. 144A, 134.